# *Supporting information for:*

## Enhanced Water Permeation through Terahertz-Induced Phase and Diffusion Transition in Metal-Organic Framework Membrane

Zhi Zhu[1], Lei Wang[1], Shaojian Yan[1], Qilin Zhang[2*], Hui Yang[3*]

*[1] Key Laboratory of Optical Technology and Instrument for Medicine, Ministry of Education, College of Optical-Electrical and Computer Engineering, University of Shanghai for Science and Technology, Shanghai 200093, China*

*[2] School of Mathematics, Physics and Finance, Anhui Polytechnic University, Wuhu 241000, China*

*[3] The Medical Instrumentation College of Shanghai University of Medicine & Health Sciences, Shanghai 201318, China*

*\*Email: hellozhangql@163.com, yangh_23@sumhs.edu.cn*

## Contents

# 1. Details of simulations
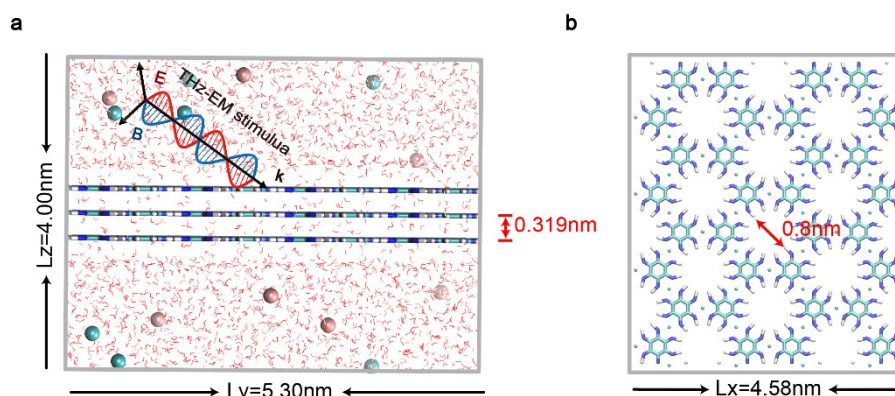
## 1.a Simulation parameters and methods



**FIG. S1. Schematic of a typical simulation box which is consisted of three layers of Cu-HAB MOF material, where (a) and (b) correspond to the side and top views, respectively. For multiple layers membranes, the distance between each layer is 0.319 nm and all layers are fully aligned, the pore diameter is measured to be approximately 0.8 nm. The green and red balls represent the Na and Cl ions in the box, respectively. The red and blue arrows indicate the electric and magnetic components of the EM stimulus, respectively. Water molecules (short red lines) pass through the three-layer MOF membrane along the *z*-direction.**

As shown in Fig. S1, MOF membrane consists of three layers of two-dimensional (2D) Cu-HAB MOF stacked in parallel. All atoms in the MOF membrane were characterized by the Lennard-Jones parameters with a potential well depth ($\varepsilon$) and a van der Waals radius ($\sigma$) (Tab. S1) [1]. The number of water molecules was 2809, and the number of Na and Cl ions was 7. The OPLS/AA force field [2] was used to deal with the interaction between atoms, where the Lennard-Jones parameters of different atoms are calculated based on the geometric average method, and the hopping frog algorithm is used to solve the particle equation of motion. During the simulation, we employed the NPT ensemble to pre-equilibrate all simulation systems. After reaching equilibrium, the NVT ensemble was employed to conduct the production run, with the system temperature maintained at 300 K using the Nose-Hoover thermostat during the application of electromagnetic stimulation (Fig. S2). The particle-mesh-Ewald (PME) method [3] was used to treat the electrostatic interaction, and the cutoff radius of the electrostatic and van der Waals interaction was 1 nm. Each simulation was 500 ns with a time step of 1 fs.

**Table S1.** The Lennard-Jones parameters used in simulations

| Interaction | $\sigma(\text{Å})$ | $\varepsilon(kcal/mol)$ |
|:---:|:---:|:---:|
| C-C | 3.3900 | 0.0692 |
| N-N | 3.8930 | 0.0740 |
| Cu-Cu | 2.6160 | 4.7200 |
| H-H | 0.0000 | 0.0000 |

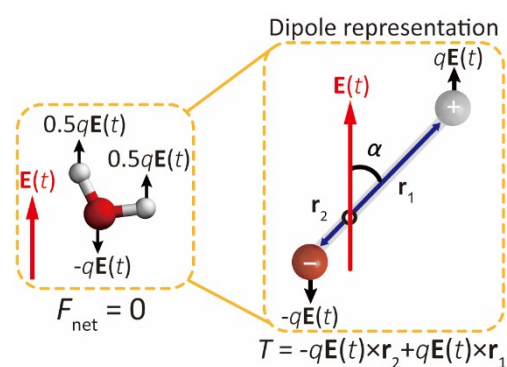## 1.b The interaction and influence of the THz electric field on the simulation system



**FIG. S2. The interaction of the electric field with the atoms in the system exerts a fluctuating force on each charged atom, thereby influencing the rotation of neutral water molecules via torque.**

The oscillating electric field interacting with the system generates an oscillating force exerted on each charged atom. During the MD simulations, if there's a change in the dipole orientation, bond angle, or bond length of a water molecule, the resultant torque experienced by the molecule will vary accordingly, despite the total electric field force on the entire molecule always being zero, as shown in Fig. S2. This fact indicates that the oscillation force on water molecules will affect the local orientations and reorganization dynamics of water molecules.
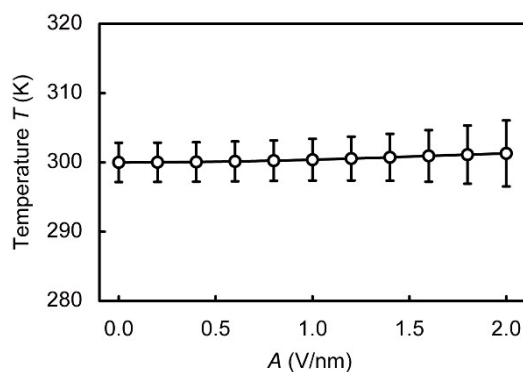
## 1.c Temperature variation of simulation systems



**FIG. S3. The temperature fluctuation of simulation systems under the 7.5 THz EM stimulus with different strengths A. All systems were maintained at an equilibrium temperature of 300 K.**

Despite the introduction of an external energy into the simulated system, the utilization of a surrounding heating bath (specifically, the Nose-Hoover thermostat) proves effective in dissipating excessive heat. Consequently, the temperature exhibits slight fluctuations as depicted in Fig. S3 but consistently hovers around 300 K.

## 1.d Identification of water molecules within MOF and details for calculating vibrational spectroscopy

We utilized molecular trajectories in simulation data to identify the water molecules within the MOF. Specifically, by processing the positional information files using custom-written scripts, we were able to determine the location and thickness of the MOF membrane in the z-direction. By restricting the selection to specific positions of water molecules within a range, we effectively identified the water molecules within the MOF membrane. Due to the short residence time of water in the 3-layer MOF membrane, which hampers the calculation of their vibrational spectra, we increased the number of membrane layers to 10 to prolong the residence time of water molecules within the membrane. Afterward, we selected water molecules in the membrane and calculated the vibration spectrum for each individual molecule, subsequently averaging them. It is worth noting that the spectral profiles of individual water molecules exhibit substantial similarity.

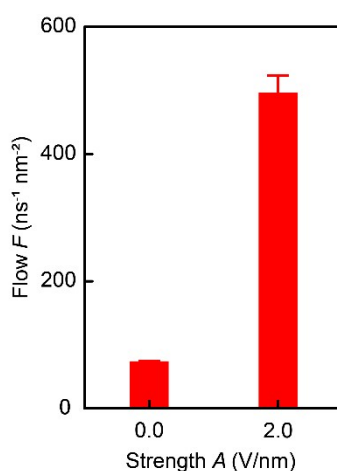## 1.e Permeation enhancement under THz influence with a rigid water model



**FIG. S4. Comparison of flow for rigid water molecule permeates through the MOF between the case without THz-EM wave and with the 7.5 THz-EM wave at the strength of 2.0 V/nm.**

Fig. S4 illustrates the comparison of flow for rigid water molecule across the MOF between the case without THz-EM wave and with the 7.5 THz-EM wave at strength $A$ = 2.0 V/nm. The water flow is $74.20 \pm 0.30$ ns$^{-1}$ nm$^{-2}$ for the case without THz-EM wave, and $496.80 \pm 26.39$ ns$^{-1}$·nm$^{-2}$ for the case with a 7.5 THz-EM wave at $A$ = 2.0 V/nm. This fact demonstrates that our conclusion, frequency-specific terahertz stimulation enhances the permeation of water in MOF, is unaffected by the choice of a rigid water model.

## 2. Effect of the polarization direction of 7.5-THz EM wave on water permeation and translational and rotational kinetic energy of water molecules within MOF
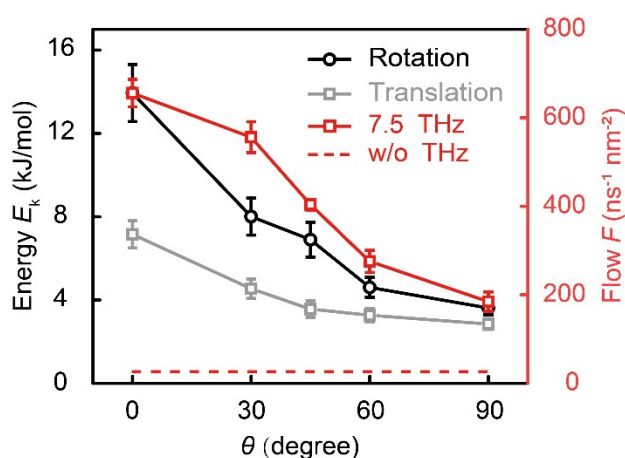


**FIG. S5. The dependence of water permeation and translational and rotational kinetic energy of water molecules within MOF membrane on the polarization direction of 7.5 THz-EM waves with strength of $A$ = 2.0 V/nm. The black and gray curves represent rotational and translational**

**kinetic energy, respectively, while the solid and dashed red curves represent water flow with and without 7.5 THz-EM, respectively.**

As depicted in Fig. S5, our computational findings illustrate the correlation between water flow $F$ and the polarization direction of the applied terahertz electric field. When the electric field shifts from being perpendicular to the membrane plane ($\theta = 0°$) to parallel ($\theta = 90°$), the flow rate decreases from $655.78 \pm 31$ ns$^{-1}$·nm$^{-2}$ to $184.59 \pm 21.90$ ns$^{-1}$·nm$^{-2}$. Moreover, the rotational and translational kinetic energy of water molecules within the MOF membrane exhibit a declining trend. This suggests that the resonance between water molecules and THz waves weakens, resulting in a reduction in the enhancement of kinetic energy and subsequently, a decline in permeability.

## 3. The effect of temperature (thermal effect) on the H-bonds number formed by a bulk water molecule or water molecule in MOF with neighboring molecules
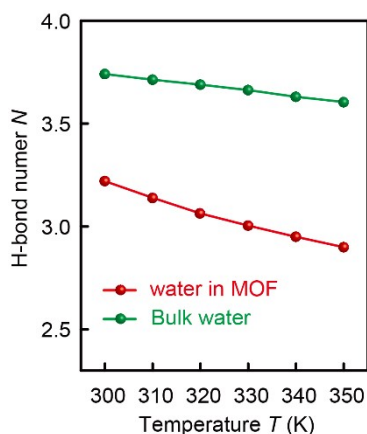


**FIG. S6. For the case without EM stimulus, the average number of H-bonds formed by a water in MOF ($N_{\text{water in MOF}}$, red ball) or bulk water molecule ($N_{\text{bulk}}$, green ball) with neighboring molecules as a function of the ambient temperature ($T$).**
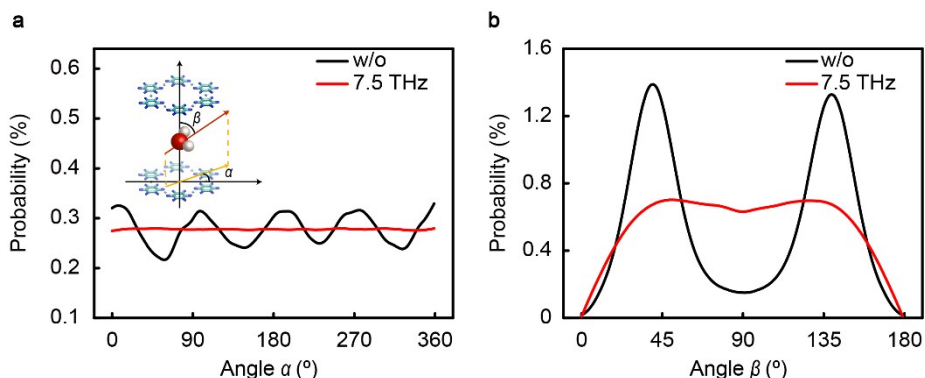
# 4. Spatial distribution of water molecules dipole



**FIG. S7. Water molecule dipole distribution probability. a)** Probability distributions of the water dipole orientations with respect to the angle $\alpha$. The strength $A = 2.0$ V/nm. Inset: the angle $\alpha$ between the projection of the water dipole onto a plane parallel to the membrane and the x-axis in the plane and the angle $\beta$ between the dipole and the direction perpendicular to the plane. **b)** Probability distributions of the water dipole orientations with respect to the angle $\beta$. The electric-component strength $A = 2.0$ V/nm.

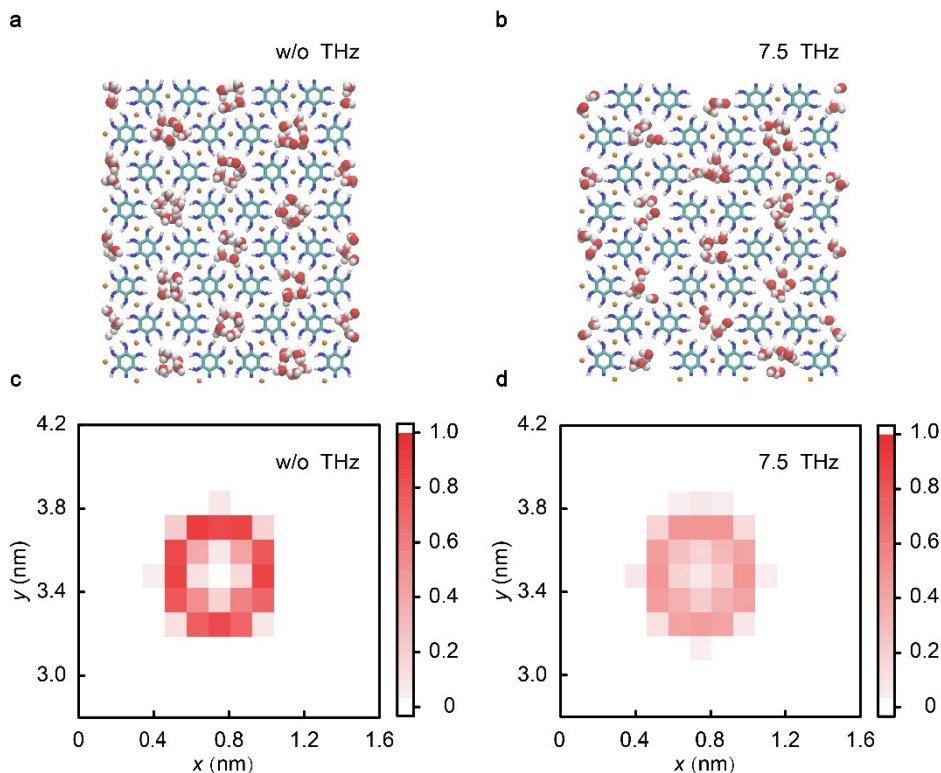# 5. The structural variation for water molecules within MOF



**FIG. S8. Structural analysis of water molecule dynamics in MOF membrane. a-b)** Snapshot comparison of water molecule structures within the MOF membrane in cases without (a) and with

THz-EM (b). **c-d)** 2D density distribution of water molecules within a single pore of the MOF membrane.

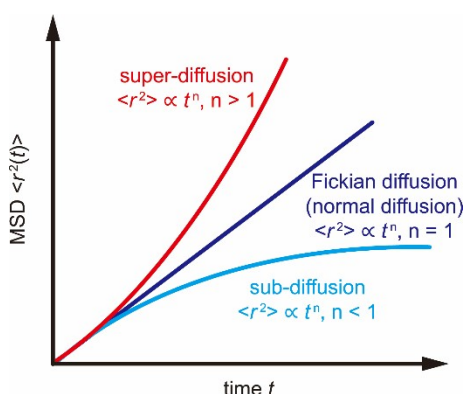## 6. Classification of diffusion types



**FIG. S9. The classification of diffusion types is based on the behavior of the slope change observed on the MSD-time curve. A constant slope suggests Fickian diffusion, while an increase and decrease correspond to super-diffusion and sub-diffusion, respectively.**

Conventionally, the classification of diffusion types is based on the exponent $n$ of the time $t$ in the mean squared displacement (MSD) equation. As shown in Fig. S9, when $n = 1$, the MSD exhibits a linear relationship with $t$, and the slope of the MSD-time curve remains constant, indicating Fickian diffusion or normal diffusion. In contrast, when $n > 1$ or $n < 1$, the MSD demonstrates a nonlinear relationship with $t$, resulting in an increase or decrease in the slope of the MSD-time curve, denoting a super-diffusion and sub-diffusion, respectively.

## References

[1]     Z. Cao, V. Liu, A. Barati Farimani, Water desalination with two-dimensional metal–organic framework membranes, *Nano Lett.* 2019, **19**, 8638-8643.

[2]     W. L. Jorgensen, D. S. Maxwell, J. Tirado-Rives, Development and testing of the OPLS all-atom force field on conformational energetics and properties of organic liquids, *J. Am. Ceram. Soc.* 1996, **118**, 11225-11236.

[3]     T. Darden, D. York and L. Pedersen, Particle mesh Ewald: An N·log (N) method for Ewald sums in large systems, *J. Chem. Phys.* 1993, **98**, 10089-10092.